VOL. 13, NO. 5, MARCH 2018 ISSN 1819-6608
ARPN Journal of Engineering and Applied Sciences

www.arpnjournals.com

TOTAL-CORROSION MODELLING AND CORROSION RATE CORRELATION FOR *Anthocleista djalonensis* LEAF-EXTRACT ADMIXED STEEL-REINFORCED CONCRETE IN 3.5% NaCl

Joshua Olusegun Okeniyi[1, 2] and Abimbola Patricia Idowu Popoola[2]
[1]Department of Mechanical Engineering, Covenant University, Ota, Nigeria
[2]Department of Chemical, Metallurgical and Materials Engineering, Tshwane University of Technology, Pretoria, South Africa
E-Mail: joshua.okeniyi@covenantuniversity.edu.ng

ABSTRACT

Assessment of admixture performance, by electrochemical monitoring techniques, on the inhibition of concrete steel-rebar corrosion in corrosive environments, has the potential challenge that simpler-to-undertake methods may not indicate absolute corrosion activity in the test-system. In this paper, total-corrosion (*TC*) was modelled, as per ASTM G109, from macrocell-current measurements, using zero-resistance ammeter (ZRA), obtained from *Anthocleista djalonensis* leaf-extract admixed steel-reinforced concrete specimens that were immersed in 3.5% NaCl, for the simulation of marine/saline environment. In addition, corrosion rate (*CR*) measurements were obtained from the steel-reinforced concrete specimens using linear-polarization-resistance (LPR) method and the mean of corrosion rate was established from the dataset for each specimen using a continuous probability distribution (Weibull distribution) function. The total-corrosion model, mean of corrosion rate and the admixture concentrations were then subjected to correlation analysis. Results showed that, in spite of the different instrumentations, the total-corrosion model combined the advantages of linearized stochastic macrocell-current measurements with excellent correlation to the corrosion rate (R^2 = 99.42%), for the plant-extract admixture concentrations. The experimental test-results and the predictions from the correlation analysis both identified the 8.33 g/L *Anthocleista djalonensis* concentration as having the optimal corrosion inhibition efficiencies: η = 98.65% (experimental model) or η = 99.00% (correlation model). The implication of these results on the use of the macrocell current technique as a comparably simpler-to-undertake corrosion monitoring method than corrosion rate is detailed in the study.

Keywords: macrocell current monitoring, total-corrosion modelling, reinforcing-steel in concrete, marine/saline simulating-environment, correlation analysis, inhibition efficiency.

1. INTRODUCTION

Corrosion of steel reinforcement in concrete by chloride ingress is a major degradation factor affecting steel-reinforced concrete materials globally. This form of corrosion has the potential to cause insidious and premature failures that may be catastrophic and, by this, culminate to loss of properties and risks to the safety of life (Bastidas *et al.*, 2015; Okeniyi *et al.*, 2015a; Budelmann *et al.*, 2014; Omotosho *et al.*, 2012; Zhang *et al.*, 2010). Chloride ion ingress in steel-reinforced concrete artificial saline water, through the use of de-icing salt in temperate countries, or from natural-marine water (sea-water), in coast regions, is deleterious to steel rebar. This is because the ingress of chloride ion into the concrete initiates and promotes accelerated corrosion of the rebar while the ion itself is not consumed (Wei *et al.*, 2013). This necessitates the need for corrosion protection methods, and the evaluation of the effectiveness of those methods of mitigating corrosion, to ensure durability of steel-reinforced concrete in their service-environments.

It is widely accepted that corrosion inhibitor admixture usage is a method that offers the most effective technical and economic advantages for tackling chloride induced corrosion of reinforcing steel (Okeniyi *et al.*, 2015b; Fei *et al.*, 2014; Liubin *et al.*, 2011). For this corrosion protection method, the corrosion mitigating effectiveness can be evaluated using non-destructive electrochemical monitoring techniques (Okeniyi *et al.*, 2015c; Fei *et al.*, 2014; Liubin *et al.*, 2011). Challenges proceeding from the use of inhibitor admixtures include environmental considerations, which has led to restrictions on the use of well-known, highly effective inhibitors that are also toxic and environmentally-hazardous synthetic chemicals (Okeniyi *et al.*, 2017; Zhou *et al.*, 2012; Liubin *et al.*, 2011). This fosters the need for replacing the toxic inhibiting materials with eco-friendlier alternatives (Zhou *et al.*, 2012). This search for novel corrosion inhibiting substances creates the extra responsibility, for construction stakeholders, of ascertaining the effectiveness of the inhibitor substances for concrete steel-rebar corrosion by chloride ion ingress (Fei *et al.*, 2014). Many non-destructive electrochemical monitoring techniques are available for querying the corrosion status of reinforcing steel embedment in concrete. However, each monitoring technique exhibits its own peculiar shortcoming, which instigates the requirement for complementing one technique with another (Song and Saraswathy, 2007; Broomfield, 2003). Difficulties identified in studies on non-destructive electrochemical monitoring techniques include the fact that none of them is indicative of the complete corrosion condition (ASTM G16-13; Birbilis and Cherry, 2005; Roberge, 2003). In addition, the electrochemical techniques can exhibit random variations in data, which could mask underlying fundamental

changes in the monitored system (Birbilis and Cherry, 2005). Also, some electrochemical techniques cannot be used to represent another, due to a lack of correlation between the techniques (Gulikers, 2010; Song and Saraswathy, 2007). Suggestions from ASTM G16-13 and from literature (Okeniyi *et al.*, 2015d; Birbilis and Cherry, 2005; Roberge, 2003) indicate that analysing the data shows the potential of leading to more meaningful conclusions on the prevailing corrosion condition in a corrosive system.

Macrocell current measurement is an electrochemical monitoring technique that is often used by corrosion stakeholders because the measuring process of the technique is technically simple to undertake (Okeniyi *et al.*, 2016a; Ismail *et al.*, 2015; Okeniyi *et al.*, 2015d; Li *et al.*, 2010; McCarter and Vennesland, 2004). However, the galvanic current from this method is identified with the setback that it only measures a fraction of the corrosion activity (Ismail *et al.*, 2015; Li *et al.*, 2010; McCarter and Vennesland, 2004). According to literature (Berke and Hicks, 2004), this setback could make measurements from the method lead to misleading conclusions on the prevailing corrosion activity in given test-system. It is believed that the reason for this is most probably related to the stochastically randomised scatter, identified in ASTM G16-13 and in corrosion reports (Roberge, 2003), of corrosion test-results ensuing from the use of the method. These culminate in measured values that could both deviate from expected values of condition present in the corrosive system and, by such deviations, make interpretation of the corrosion test-results difficult. Requisite analyses may be required (ASTM G16-13; Birbilis and Cherry, 2005). Such necessity for analyses could be recognised by noting, for instance, that integration of macrocell current measurements over time indicates the total-corrosion in a corrosive system (ASTM G109-07; Berke and Hicks, 2004). Such forms of analysed macrocell current measurements has made the method useful for detailing inhibitor performance on concrete steel reinforcement corrosion in studies (Okeniyi *et al.*, 2015d; Okeniyi *et al.*, 2015e; Berke and Hicks, 2004). In one of these cited works (Okeniyi *et al.*, 2015e), analysed total-corrosion from macrocell current as per ASTM G109-07 corroborated analysed corrosion rate measurements. By that corroboration, a meaningful conclusion of admixture performance of *Morinda lucida*, a plant extract, was attained. This engenders interest for the investigation, being undertaken in this study, on the correlation obtainable from analysed total-corrosion model and the corrosion-rate. Such correlation will be useful either for utilizing macrocell current as a simpler-to-undertake electrochemical technique for assessing corrosion activity just as corrosion rate or for complementing corrosion rate measurement.

Anthocleista djalonensis (*A. djalonensis)* A. Chev Loganiaceae is a natural plant rich in safe biochemical phyto-constituents (Okeniyi *et al.*, 2014a; Bassey *et a*l, 2005) that have been characterised with N-, O- and π-electron containing ligands. Through these natural-plant attributes, the corrosion inhibition performance of extracts from it had been investigated in studies (Okeniyi *et al.*, 2016b; Okeniyi *et al.*, 2016c; Okeniyi *et al.*, 2014a; Adeyemi and Olubomehin, 2010). In spite of these, however, there are also needs for more studies on the plant's inhibition potency, especially in chloride-contaminated environment of steel-reinforced concrete immersion. The foregoing considerations constitute the motivation for investigating the relationship between the macrocell current and corrosion rate measured from steel-reinforced concrete admixed with the plant extract. There is no study in literature whereby such investigation has been done on *A. djalonensis* leaf-extract mixed into steel-reinforced concretes that were immersed in chloride-contaminated medium. This paper, therefore, employs investigation of the correlation obtainable from the total-corrosion model and the analysed corrosion-rate for detailing corrosion inhibition performance of *A. djalonensis* leaf-extract mixed into 3.5% NaCl-immersed steel-reinforced concrete.

2. EXPERIMENTAL PROCEDURE

2.1 Experimental materials

Fresh leaves of *A. djalonensis* were collected, authenticated (voucher FHI. No. 109496, from Forestry Herbarium Ibadan, Nigeria) and processed for concrete mixing/admixture as detailed in reported work (Okeniyi *et al.*, 2014a), in which the obtained leaf-extract had also been characterised using FTIR (Fourier transform infrared spectroscopy) techniques.

Concrete blocks (100 mm × 100 mm × 200 mm) having different concentrations of the *A. djalonensis* leaf-extract, were cast following prescriptions designated in ASTM C192/192M-16a and detailed in studies (Okeniyi *et al.*, 2013a; Okeniyi *et al.*, 2013b). The admixture design in this work employed six different concentrations of *A. djalonensis* leaf-extract. These concentrations ranging from 0.0 g/L (for control specimens) up to 8.33 g/L in increments of 1.67 g/L, of the concrete mixing water, in duplicates (that were tagged as "_Dup" hereafter) of steel-reinforced concrete specimens (Corbett, 2005; Dean, 2005). These culminated in a total of 12 specimens of steel-reinforced concretes for the study. Lengths of 190 mm steel-reinforcement, of diameter 12 mm, which had been subjected to uniform surface treatment as per ASTM G109–07, were employed as embedment in each steel-reinforced concrete specimen. This was such that 150 mm of the steel-reinforcement embedment was in the concrete while 40 mm of it protruded out of the concrete for electrochemical connection.

2.2 Experimental setup

Steel-reinforced concrete specimens were immersed in 3.5% NaCl-containing plastic bowls, both for accelerating rebar corrosion (Li *et al.*, 2010) and for simulating a marine/saline environment (Okeniyi *et al.*, 2015f; Okeniyi *et al.*, 2014b; Mennucci *et al.*, 2009). From each of the specimens, two different types of electrochemical measurements were obtained. These included macrocell current measurements using

Cu/CuSO4 reference electrode (CSE) and zero resistance ammeter, ZRA (Okeniyi *et al.*, 2015g; Abdelaziz *et al.*, 2009; McCarter and Vennesland, 2004), as per ASTM G109-07, and corrosion rate measurements using a 3-electrode linear polarization resistance (LPR) instrument (Okeniyi *et al.*, 2013b; Okeniyi *et al.*, 2013c). These measurements were taken in five-day intervals, first, for 40 days and, thereafter, in seven-day intervals for the seven weeks following. These constitute 89 days of steel-reinforced concrete immersion test-experiments from which n = 16 number of data points were obtained for each of the two employed electrochemical monitoring techniques for the work in this report.

2.3 Computations for experimental data

Total-Corrosion modelling: Total-corrosion modelling employs discrete integration of the macrocell current measurements over the period for the experiment using the expression from ASTM G109-07 that is given by Equation (1) (Okeniyi *et al.*, 2015g).

$$TC_{\kappa} = TC_{\lambda-1} + \left[\left(t_{\lambda} - t_{\lambda-1}\right) \times \left(i_{\lambda} + i_{\lambda-1}\right)/2\right]; \;\; \lambda = 2,\ 3,\ ...,\ n \quad (1)$$

Where: TC is the total-corrosion (C); t is the time (s) elapsed between the previous, (λ–1), macrocell current measurement $i_{\lambda-1}$ (A), at time $t_{\lambda-1}$, and the present, (λth), macrocell current measurement i_{λ} (A) at time t_{λ}.

Corrosion rate analysis: Measurements of corrosion rate, CR (mm/y), were subjected to the analyses of the Normal and Weibull probability distribution functions (PDF) (Okeniyi *et al.*, 2014c; Okeniyi *et al.*, 2014d). The Normal model of corrosion rate test-data employed well-known expression detailed in literature (Okeniyi *et al.*, 2014a; Dean, 2005), while the Weibull model employed the linear expression in Equation (2) (Okeniyi *et al.*, 2015h; Dean, 2005).

$$\ln[-\ln[1-P(x)]] = c\ln(x) - c\ln(b) \quad (2)$$

Where x is the corrosion rate test-data variable, b and c are, respectively, the Weibull scale and shape parameters, and $P(x)$ is the Weibull cumulative distribution function (CDF) given by Equation (3) (Okeniyi *et al.*, 2015h; Okeniyi *et al.*, 2014c).

$$P(x) = 1 - \exp\left[-\left(\frac{x}{b}\right)^{c}\right] \quad (3)$$

Weibull estimation of mean corrosion rate, μ, was then obtained from Equation (4).

$$CR_{mean} \equiv \mu = b\Gamma\left(1 + \frac{1}{c}\right) \quad (4)$$

As recommended in ASTM G16-13 and in corrosion texts (Roberge, 2005; Roberge, 2003), the scattering of the corrosion rate test-data like the Weibull PDF, was studied via usage of the Kolmogorov-Smirnov (K-S) goodness-of-fit test-statistics at the test-criteria of α = 0.05 significant level (Okeniyi *et al.*, 2015i; Okeniyi and Okeniyi, 2012).

Correlation analyses were done in the study by subjecting different relationship fittings of the requisite parameters for the analyses to the coefficient of determination and analyses of variance (ANOVA) modelling (Okeniyi *et al.*, 2014a; Okeniyi *et al.*, 2014c). These experimental parameters include usage of the total-corrosion and *A. djalonensis* leaf-extract concentration, as variables that are dependent on the corrosion rate, which in turn was employed as the independent variable in the course of the correlation modelling analyses. By these analyses, a correlated relationship was identified, which by statistical inference showed that there exists a relationship between the independent and dependent variables at α = 0.05 level of significance. From the results of the analyses, the experimental and mathematically correlated predictions of corrosion rate were applied for estimating the inhibition efficiency details of the *A. djalonensis* leaf-extract performance on concrete steel-rebar corrosion through Equation (5) (Okeniyi *et al.*, 2015f; Okeniyi *et al.*, 2013a; Okeniyi *et al.*, 2013b).

$$\eta(\%) = \frac{CR_{control} - CR_{admixed}}{CR_{control}} \times 100 \quad (5)$$

3. RESULTS

3.1 Analyses of measured corrosion datasets

The results of the macrocell current and corrosion rate measurements through the experimental period are plotted in Figure-1, wherein Figure-1(a) shows plots of macrocell current, and Figure-1(b) the plots for corrosion rate. The Figure exemplifies stochastically randomised data, conforming to the inferences from corrosion standard (ASTM G16-13) and text (Roberge, 2003), and that could make interpretations of the corrosion test-results difficult. Despite these observable randomisations, the macrocell current and the corrosion rate measurements of the duplicates of control samples were both higher than the macrocell current and corrosion rate of the other specimens admixed with *A. djalonensis*. The exceptions to this are just some spikes in the corrosion rate from a few *A. djalonensis* admixed steel-reinforced concrete specimens. These exceptions from the measurements of corrosion rate data could be due to instances of deviation from the expected results of corrosion conditions that are prevalent in their test-systems.

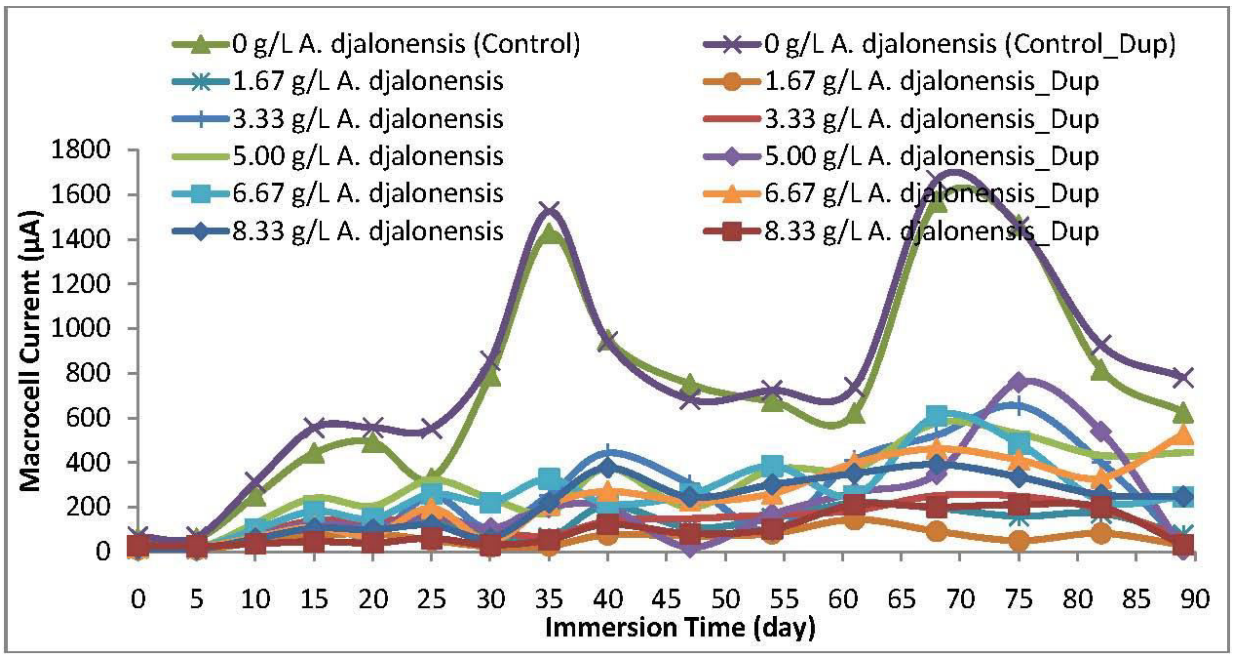

(a)

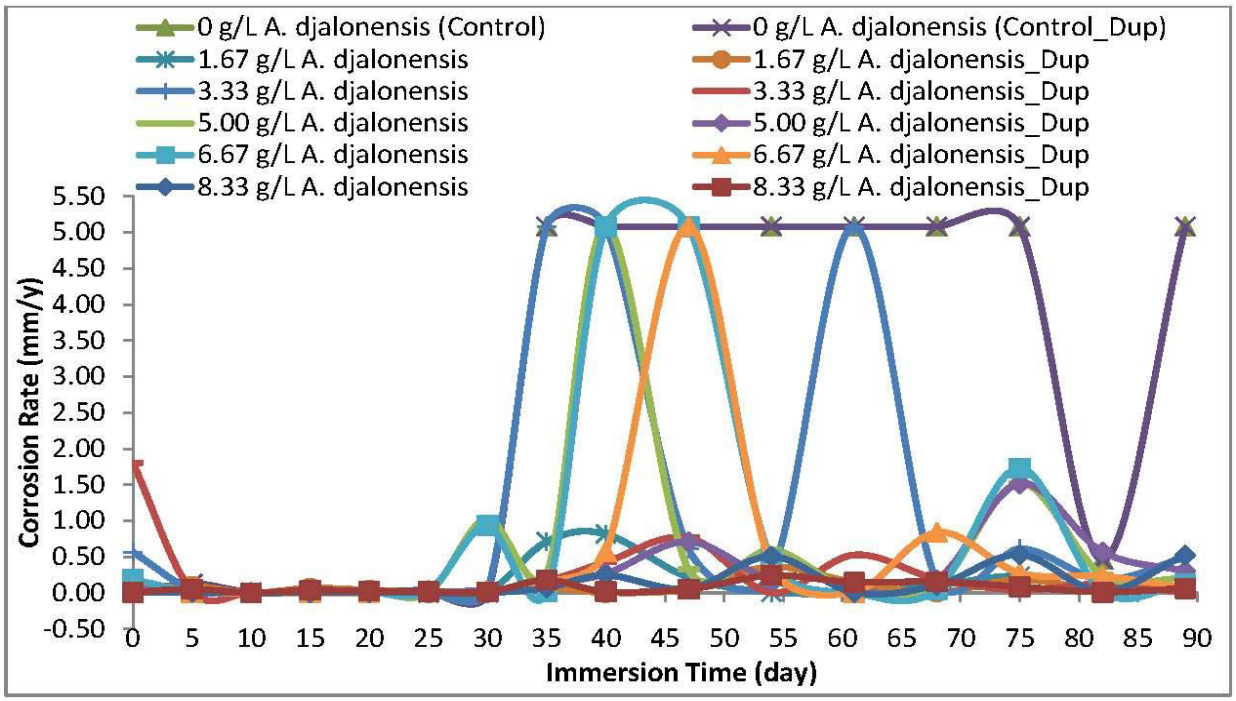

(b)

Figure-1. Plots of measured corrosion test-data (a) macrocell current (b) corrosion rate.

3.2 Kolmogorov-Smirnov Goodness-of-Fit (K-S GoF) tests of the Scatter of Corrosion Datasets

Prior to statistical distribution detailing of corrosion rate test-results, it is important to ascertain whether the corrosion rate data scattered like each of the PDF fittings or not. The results of the test-statistics for this, the Kolmogorov-Smirnov (K-S) *p*-values, are plotted in Figure-2. The plots in the figure also contain the line K-S *p*-value = α = 0.05 level of significance for the direct identification of dataset(s) that distributed (and those that were not distributed) like each of the PDF models from the figure. The plots, therefore, show that six datasets of corrosion rate, including the controls, out of 12 datasets were not scattered like the Normal, i.e. K-S *p*-values < 0.05. In contrast, all corrosion rate datasets in the study followed the Weibull PDF in accordance to the K-S GoF test-criteria. These Weibull PDF compatible datasets exhibited K-S *p*-values that were surpassed 0.05. Thus, by these result trends, usage of the Weibull PDF is supported for detailing the test-results of corrosion rate in this work.

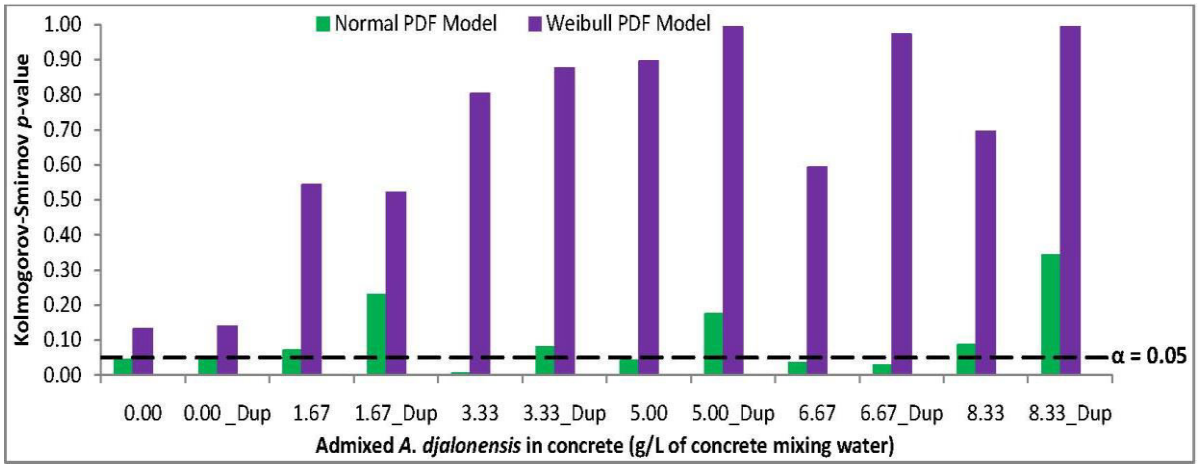

Figure-2. Kolmogorov-Smirnov testing of the corrosion rate datasets scatter like the PDF fittings.

3.3 Analysed Models of Results from Corrosion Testing

The modelled results from corrosion testing in the study are plotted in Figure-3. These include the total-corrosion model, from macrocell current measurements, in Figure-3(a), while the mean model of corrosion rate via using the models of Normal pdf (for comparison) and of Weibull pdf, are shown in Figure-3(b).

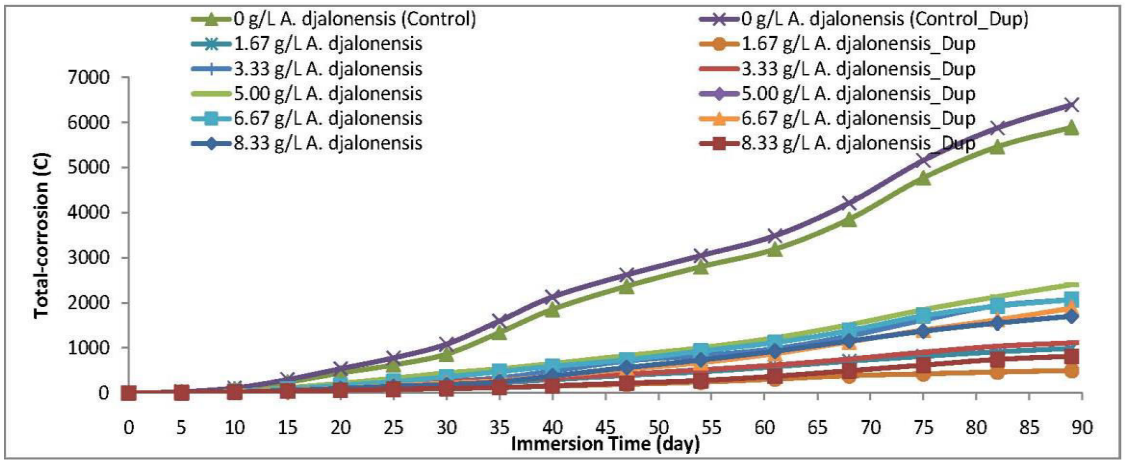

(a)

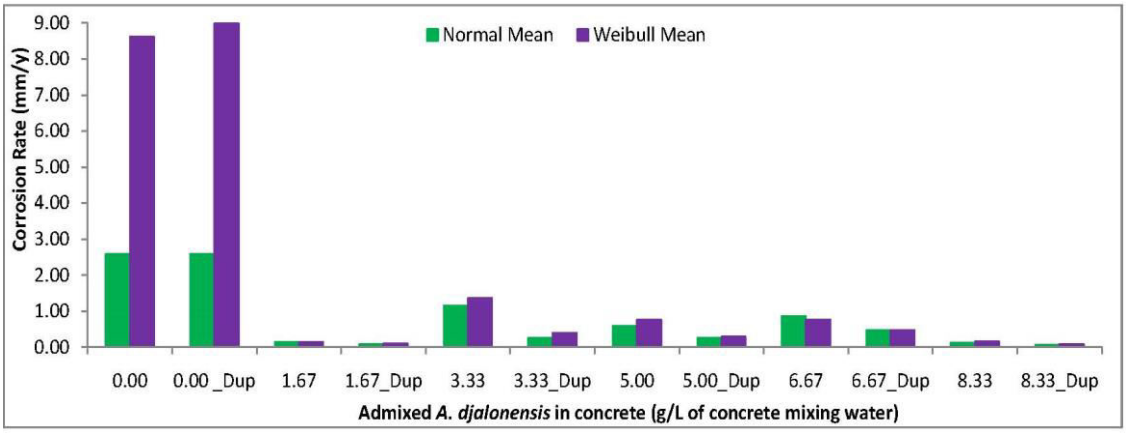

(b)

Figure-3. Analysed models of corrosion tests (a) Total-Corrosion (b) Corrosion rate.

The plots in the figure show that the requisite analyses instil order and, consequently, ease of interpretation to the corrosion test-results. For instance, it could be observed from Figure-3(a) that the total-corrosion

modelling facilitates linearization of the previously stochastic plots of macrocell current, when compared to Figure-1(a). In addition, the agreements in corrosion rate values between duplicates of steel-reinforced concretes having the same *A. djalonensis* leaf-extract concentrations, exhibited better clarity in Figure-3(b) than in Figure-1(b). It is also deductible from Figure-3(b) that the Weibull mean model of corrosion rate PDF highly over-predicted the Normal mean model of this same corrosion test-variable. However, the K-S goodness-of-fit tests in Figure-2 show that the distribution of the corrosion rate datasets followed the Weibull PDF. This indicates that the Weibull models of corrosion rate portray the prevalent value expectations in the corrosion test-systems, but from which the measured data had deviated.

3.4 Correlation fitting model analyses

The total-corrosion and corrosion rate models exhibited agreement in that both were highly reduced in the steel-reinforced concrete samples admixed with *A. djalonensis* leaf-extract in comparison with the control specimens. This indicates that there could be some form mathematical expression relating the corrosion-rate (*CR*) and total-corrosion (*TC*) for the concentration, ρ, of *A. djalonensis* leaf-extraction admixtures, in the studied steel-reinforced concretes. Therefore, several relationship models were investigated through coefficient of determination and ANOVA modelling. From these were obtained the correlation fitting expression in Equation (6).

$$CR = -6.3\times10^{-2}\left(\rho + 1.033\times10^{4} + 0.63TC - 6.537\times10^{2}\sqrt{TC} + 5.829\times10^{3}\sqrt[3]{TC} - 0.122\times10^{5}\sqrt[5]{TC}\right) \quad (6)$$

This mathematical fitting expression in Equation (6) can be written compactly in the form shown in Equation (7).

$$CR = -6.3\times10^{-2}\left(\rho + a_0 + \sum_{k=1}^{5} a_k \times 10^{k}\cdot TC^{\frac{1}{k}}\right) \quad (7)$$

Where a_k (k = 0, 1, 2, …, 5) are numerical constants. For this mathematically fitted correlation, the coefficient of determination, R^2 = 99.42%, which classifies as "excellent" efficiency model, according to the efficiency model classification from a reported study (Coffey *et al.*, 2013). It is worth noting that the root expressions that are similar with the correlation fitting obtained in this study had been derived also in the literature (Izquierdo *et al.*, 2004) between values of potential and thresholds of chloride ingress for concrete steel-rebar depassivation.

Results of analysis of variance application to the mathematically fitted correlations of Equations (6) and (7) are as shown in Table-1. This shows that the ANOVA *p*-value = 0.000001 for the correlation fitting model. It is worth noting that this *p*-value is less than α = 0.05 level of significance. Therefore, for the studied concentrations of *A. djalonensis,* there is significant relationship between the corrosion rate, that were measured via utilising the LPR instrument and the total-corrosion, obtained from macrocell current measured through a ZRA instrument.

Table-1. ANOVA (Analysis of Variance) from the mathematically fitted correlation.

Source of variation	*df*	SS	MS	F	*p*-value
Regression	5	116.8963	23.3793	205.3888	0.000001
Residual	6	0.6830	0.1138		
Total	11	117.5793			

3.5 Inhibition efficiency from the experimental and correlation fitting models

By applying Equation (5) to the experimental and correlated prediction of corrosion rate for each specimen of steel-reinforced concrete samples facilitate inhibition efficiency modelling. From these, computed results of the corrosion inhibition efficiency on steel-reinforcement, averaged over each duplicate of *A. djalonensis* admixed steel-reinforced concretes, are presented in Figure-4. The figure shows very keen agreement between the experimental and mathematically correlated prediction models of corrosion inhibiting effectiveness. The figure also indicates that the *A. djalonensis* leaf-extract concentrations exhibited excellent inhibition efficiency performance on steel-reinforcement corrosion in concrete immersed in the 3.5 NaCl medium, the saline/marine simulating-environment. All the admixtures exhibited η > 90% inhibition effectiveness performance both by the experimental and by the mathematically correlated prediction models. This inhibition efficiency performance surpasses the reported performance for the bark extract of this plant on aluminium corrosion protection in acidic sulphate medium by other researchers (Adeyemi and Olubomehin, 2010). It was also established in this study that the 8.33 g/L *A. djalonensis* leaf-extract concentration exhibited the best inhibition efficiency, η = 98.65% (experimental model) or η = 99.00% (correlation fitting model). In furtherance of comparisons, the best inhibition efficiency effectiveness by experimental and correlated models from this study still surpasses that obtained from such models on $NaNO_2$ admixture from a recently reported work (Okeniyi *et al.*, 2015f).

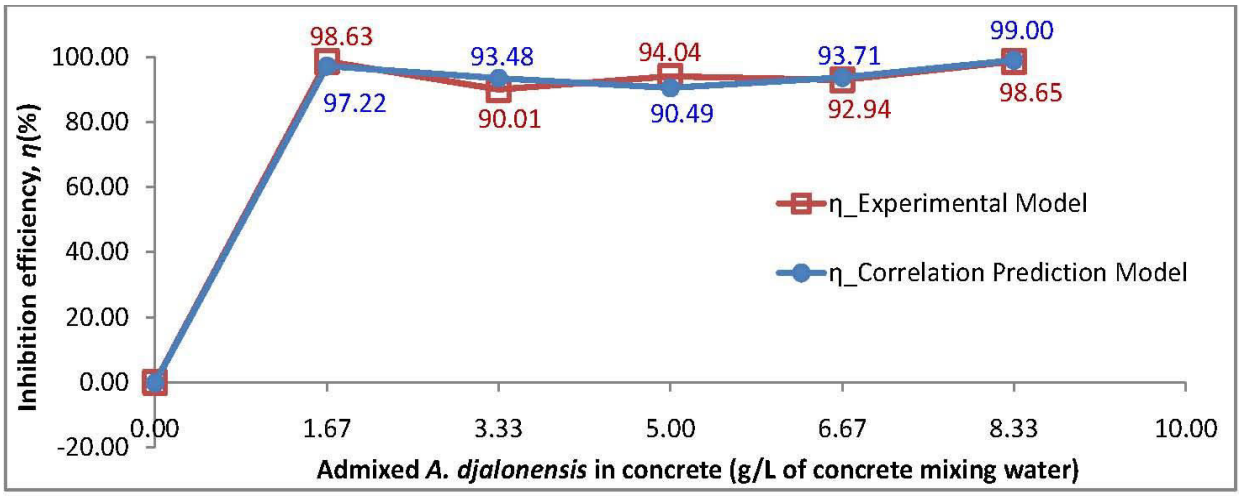

Figure-4. Experimental and mathematically correlated prediction models of inhibition efficiencies.

The excellent correlation fitting between experimental parameters in the study and agreements between experimental and correlation performance predictions has implications on corrosion monitoring technique usage that is simpler-to-undertake instead of the LPR technique. For instance, it is well known that the impressed current perturbation from the LPR technique can induce pitting corrosion on the metallic material to which the corrosion monitoring technique is applied. This, in contrast, exemplifies the simplicity of the macrocell current measurement, from which total-corrosion is analysed, because this corrosion monitoring technique exhibited no such perturbation on the metallic specimen. Because the method of macrocell current monitoring is a non-perturbation technique, no damage is incurred on the metallic specimen, from which the macrocell current measurements are obtained. These constitute reasons by which it is considered that this correlation modelling approach from this study could go a long way in predicting prevalent corrosion activity/conditions in steel-reinforced concrete designed for aggressive media. This also will facilitate the use of the total-corrosion technique for assessing performance of corrosion protection methods such as novel or well-known corrosion inhibitor usage in steel-reinforced concrete designed for corrosive service-environment.

4. CONCLUSIONS

The total-corrosion model, as per ASTM G109, facilitated linearization of the stochastic macrocell current measurements, and correlated excellently with the corrosion rates from LPR technique in detailing *A. djalonensis* leaf-extract performance on steel-reinforcement corrosion in 3.5% NaCl-immersed concrete. Prediction from the excellently correlated fitting model, R^2 = 99.42%, highly agreed with the experimental model on corrosion inhibition efficiency performance of *A. djalonensis* leaf-extract in the steel-reinforced concretes immersed in 3.5% NaCl. By these data-modelling agreements, 8.33 g/L *A. djalonensis* admixture concentration, in steel-reinforced concrete, exhibited optimal corrosion-inhibition efficiency performance, η = 98.65% by the experimental or η = 99.00% by the correlation prediction model. All these are in spite of the different instrumentations for the two corrosion-monitoring techniques employed in the study. By these results, it is concluded that the total-corrosion monitoring method exhibited potential of an approach that is simpler-to-undertake, instead of corrosion rates obtained from the LPR technique. This simpler-to-undertake technique can then find usefulness and applications for predicting prevailing corrosion conditions and assessing the effectiveness of corrosion protection techniques, including inhibitor usage, in steel-reinforced concretes designed for usage in the saline/marine environment.

ACKNOWLEDGEMENT

Authors appreciate part-funding and supports for this research work by the following institutions: The National Research Foundation – The World Academy of Sciences, NRF-TWAS, [Grant No: 105552], and Covenant University Centre for Research Innovation and Discovery, CUCRID, Covenant University, Ota, Nigeria.

REFERENCES

Abdelaziz G.E., Abdelalim A.M.K. and Fawzy Y.A. 2009. Evaluation of the short and long-term efficiencies of electro-chemical chloride extraction. Cem. Concr. Res. 39(8): 727-732.

Adeyemi O.O. and Olubomehin, O.O. 2010. Investigation of *Anthocleista djalonensis* stem bark extract as corrosion inhibitor for Aluminum. The Pac. J. Sci. Technol. 11(2): 455-462.

ASTM C192/C192M-16a 2016. Standard Practice for Making and Curing Concrete Test Specimens in the Laboratory, ASTM International, West Conshohocken, PA.

ASTM G109-07 2013. Standard Test Method for Determining Effects of Chemical Admixtures on Corrosion of Embedded Steel Reinforcement in Concrete Exposed to Chloride Environments, ASTM International, West Conshohocken, PA.

ASTM G16-13 2013. Standard Guide for Applying Statistics to Analysis of Corrosion Data. ASTM International, West Conshohocken, PA.

Bassey A.S., Okokon J.E., Etim E.I., Umoh F.U. and Bassey E. 2009. Evaluation of the in vivo antimalarial activity of ethanolic leaf and stembark extracts of *Anthocleista djalonensis*. Indian J. Pharmacol. 41(6): 258-261.

Bastidas D.M., Criado M., Fajardo S., La Iglesia A. and Bastidas J.M. 2015. Corrosion inhibition mechanism of phosphates for early-age reinforced mortar in the presence of chlorides. Cem. Concr. Compos. 61: 1-6.

Berke N.S. and Hicks M.C. 2004. Predicting long-term durability of steel reinforced concrete with calcium nitrite corrosion inhibitor. Cem Concr Compos. 26(3): 191-198.

Birbilis N. and Cherry B.W. 2005. Monitoring the corrosion and remediation of reinforced concrete on-site: An alternative approach. Mater. Corros. 56(4): 237-243.

Broomfield J.P. 2003. Corrosion of steel in concrete: understanding, investigation and repair. New York: Taylor & Francis.

Budelmann H., Holst A. and Wichmann H. J. 2014. Non-destructive measurement toolkit for corrosion monitoring and fracture detection of bridge tendons. Struct. Infrastruct. Eng. 10(4): 492-507.

Coffey R., Dorai-Raj S., O'Flaherty V., Cormican M. and Cummins E. 2013. Modeling of pathogen indicator organisms in a small-scale agricultural catchment using SWAT. Hum. Ecol. Risk Assess.: An Int. J. 19(1): 232-253.

Corbett R.A. 2005. Immersion Testing. In: Baboian, R. (ed.), Corrosion Tests and Standards: Application and Interpretation, 2nd ed., ASTM International, West Conshohocken, PA, 139-146.

Dean S.W. 2005. Statistical Treatment of Data, Data Interpretation, and Reliability. In: Baboian, R. (ed.), Corrosion Tests and Standards: Application and Interpretation, 2nd ed., ASTM International, West Conshohocken, PA, 83-88.

Fei F.L., Hu J., Wei J.X., Yu Q.J. and Chen Z.S. 2014. Corrosion performance of steel reinforcement in simulated concrete pore solutions in the presence of imidazoline quaternary ammonium salt corrosion inhibitor. Constr. Build. Mater. 70: 43-53.

Gulikers J. 2010. Statistical interpretation of results of potential mapping on reinforced concrete structures. Eur. J. Environ. Civ. Eng. 14(4): 441-466.

Ismail M., Raja, P.B. and Salawu A.A. 2015. Deeper understanding of green inhibitors for corrosion of reinforcing steel in concrete. In: Lim, H. (ed.), Handbook of Research on Recent Developments in Materials Science and Corrosion Engineering Education. IGI Global, Hershey, PA. 118-146.

Izquierdo D., Alonso C., Andrade C. and Castellote M. 2004. Potentiostatic determination of chloride threshold values for rebar depassivation: experimental and statistical study. Electrochim. Acta. 49(17): 2731-2739.

Li L., Dong S., Wang W., Hu R., Du R., Lin C., Zhuo X. and Wang J. 2010. Study on interaction between macrocell and microcell in the early corrosion process of reinforcing steel in concrete. Sci. China Technol. Sci. 53(5): 1285-1289.

Liubin S., Daowu Y., Sanjun P., Yuchun L. and Cong L. 2011. Electrochemical study of inhibitors to improve the anti-corrosion performance of reinforced bar in the concrete. Anti-Corrosion Methods and Materials. 58(1): 22-25.

McCarter W.J. and Vennesland Ø. 2004. Sensor systems for use in reinforced concrete structures. Constr. Build. Mater. 18(6): 351-358.

Mennucci M.M., Banczek E.P., Rodrigues P.R.P. and Costa I. 2009. Evaluation of benzotriazole as corrosion inhibitor for carbon steel in simulated pore solution. Cem. Concr. Compos. 31(6): 418-424.

Okeniyi J.O., Okeniyi E.T., Ogunlana O.O., Owoeye T.F. and Ogunlana O.E. 2017. Investigating biochemical constituents of *Cymbopogon citratus* leaf: Prospects on total corrosion of concrete steel-reinforcement in acidic-sulphate medium. In: TMS 2017 146th Annual Meeting & Exhibition Supplemental Proceedings, Springer International Publishing. 341-351.

Okeniyi J.O., Okeniyi E.T. and Owoeye T.F. 2016a. Bio-characterisation of *Solanum aethiopicum* leaf: prospect on steel-rebar total-corrosion in chloride-contaminated-environment. Prog. Ind. Ecol., An Int. J. 10(4): 414-426.

Okeniyi J.O., Loto C.A. and Popoola A.P.I. 2016b. Anticorrosion performance of *Anthocleista djalonensis* on steel-reinforced concrete in a sulphuric-acid medium. HKIE Trans. 23(3): 138-149.

Okeniyi J.O., Loto C.A. and Popoola A.P.I. 2016c. Total-corrosion effects of *Anthocleista djalonensis* and

Na_2Cr_2O7 on steel-rebar in H_2SO_4: Sustainable corrosion-protection prospects in microbial/industrial environment. In: Rewas 2016: Towards Materials Resource Sustainability. Springer International Publishing. 187-192.

Okeniyi J. O., Loto C. A. and Popoola A. P. I. 2015a. Corrosion Inhibition of Concrete Steel-Reinforcement in Saline/Marine Simulating-Environment by *Rhizophora mangle* L. Solid State Phenom. 227: 185-189.

Okeniyi J.O., Popoola A.P.I., Loto C.A., Omotosho O.A., Okpala S.O. and Ambrose I.J. 2015b. Effect of $NaNO_2$ and $C_6H_{15}NO_3$ synergistic admixtures on steel-rebar corrosion in concrete immersed in aggressive environments. Adv. Mater. Sci. Eng. 2015: Article ID 540395, p. 11.

Okeniyi J.O., Oladele I.O., Omoniyi O.M., Loto C.A. and Popoola A.P.I. 2015c. Inhibition and compressive-strength performance of $Na_2Cr_2O_7$ and $C_{10}H_{14}N_2Na_2O_8{\cdot}2H_2O$ in steel-reinforced concrete in corrosive environments. Can. J. Civ. Eng. 42(6): 408-416.

Okeniyi J.O., Omotosho O.A., Ogunlana O.O., Okeniyi E.T., Owoeye T.F., Ogbiye A.S. and Ogunlana E.O. 2015d. Investigating prospects of *Phyllanthus muellerianus* as eco-friendly/sustainable material for reducing concrete steel-reinforcement corrosion in industrial/microbial environment. Energy Procedia. 74: 1274-1281.

Okeniyi J.O., Ogunlana O.O., Ogunlana O.E., Owoeye T.F. and Okeniyi E.T. 2015e. Biochemical characterisation of the leaf of *Morinda lucida*: Prospects for environmentally-friendly steel-rebar corrosion-protection in aggressive medium. In: TMS 2015 144th Annual Meeting & Exhibition, Springer, Cham. 637-644.

Okeniyi J.O., Omotosho O.A., Loto C.A. and Popoola A.P.I. 2015f. Corrosion rate and noise resistance correlation from $NaNO_2$-admixed steel-reinforced concrete. Asian J. Sci. Res. 8(4): 454-465.

Okeniyi J.O., Omotosho O.A., Ogunlana O.O., Okeniyi E.T., Owoeye T.F., Ogbiye A.S. and Ogunlana E.O. 2015g. Investigating prospects of *Phyllanthus muellerianus* as eco-friendly/sustainable material for reducing concrete steel-reinforcement corrosion in industrial/microbial environment. Energy Procedia. 74: 1274-1281.

Okeniyi J.O., Ohunakin O.S. and Okeniyi E.T. 2015h. Assessments of wind-energy potential in selected sites from three geopolitical zones in Nigeria: Implications for renewable/sustainable rural electrification. The Sci. World J. 2015: (Article ID 581679), p. 13.

Okeniyi J.O. Okeniyi E.T., Atayero A.A. 2015i. Programming development of Kolmogorov-Smirnov goodness-of-fit testing of data normality as a Microsoft Excel® library function. J. Softw. Syst. Dev. 2015; c1-15.

Okeniyi J.O., Loto C.A. and Popoola A.P.I. 2014a. Electrochemical performance of *Anthocleista djalonensis* on steel-reinforcement corrosion in concrete immersed in saline/marine simulating-environment. Trans. Indian Inst. Met. 67(6): 959-969.

Okeniyi J.O., Loto C.A. and Popoola A.P.I. 2014b. *Morinda lucida* effects on steel-reinforced concrete in 3.5% NaCl: Implications for corrosion-protection of wind-energy structures in saline/marine environments. Energy Procedia. 50: 421-428.

Okeniyi J.O., Ambrose I.J., Okpala S.O., Omoniyi O.M., Oladele I.O., Loto C.A. and Popoola P.A.I. 2014c. Probability density fittings of corrosion test-data: Implications on $C_6H_{15}NO_3$ effectiveness on concrete steel-rebar corrosion. Sadhana. 39(3): 731-764.

Okeniyi, J.O., Loto, C.A. and Popoola, A.P.I. 2014d. Corrosion inhibition performance of *Rhizophora mangle* L bark-extract on concrete steel-reinforcement in industrial/microbial simulating-environment. International Journal of Electrochemical Science. 9(8): 4205-4216.

Okeniyi J.O., Oladele I.O., Ambrose I.J., Okpala S.O., Omoniyi O.M., Loto C.A. and Popoola A.P.I. 2013a. Analysis of inhibition of concrete steel-rebar corrosion by $Na_2Cr_2O_7$ concentrations: Implications for conflicting reports on inhibitor effectiveness. J. Cent. South Univ. 20(12): 3697-3714.

Okeniyi J.O., Omoniyi O.M., Okpala S.O., Loto C.A. and Popoola A.P.I. 2013b. Effect of ethylenediaminetetraacetic disodium dihydrate and sodium nitrite admixtures on steel-rebar corrosion in concrete. Eur. J. Environ. Civ. Eng. 17(5): 398-416.

Okeniyi J.O., Idemudia J.A., Oladele I.O., Loto C.A. and Popoola P.A.I. 2013c. Electrochemical performance of sodium dichromate partial replacement models by triethanolamine admixtures on steel-rebar corrosion in concretes. Int. J. Electrochem. Sci. 8(8): 10758-10771.

Okeniyi J.O. and Okeniyi E.T. 2012. Implementation of Kolmogorov-Smirnov P-value computation in Visual Basic®: implication for Microsoft Excel® library function. J. Stat. Comput. Simul. 82(12): 1727-1741.

Omotosho O.A., Okeniyi J.O., Ajayi O.O. and Loto C.A. 2012. Effect of synergies of $K_2Cr_2O_7$, K_2CrO_4, $NaNO_2$ and aniline inhibitors on the corrosion potential response of steel reinforced concrete in saline medium. Int. J. Environ. Sci. 2(4): 2346-2359.

Roberge P.R. 2005. Computer based data organization and computer applications. In: Baboian, R. (ed.), Corrosion Tests and Standards: Application and Interpretation, 2nd

ed., ASTM International, West Conshohocken, PA, 89-104.

Song H.W. and Saraswathy V. 2007. Corrosion monitoring of reinforced concrete structures-A. Int. J. Electrochem. Sci, 2: 1-28.

Roberge P.R. 2003. Statistical Interpretation of Corrosion Test Results. In: Cramer, S.D. and Covino Jr., B.S. (eds.), ASM handbook, Vol. 13A - Corrosion: Fundamentals, Testing, and Protection. ASM International, Materials Park, OH, 425-429.

Wei J., Dong J.H. and Ke W. 2013. Corrosion evolution of scaled rebar in concrete under dry/wet cyclic condition in 3.5% NaCl solution. Int. J. Electrochem. Sci. 8: 2536-2550.

Zhang J., Wang J. and Kong D. 2010. Chloride diffusivity analysis of existing concrete based on Fick's second law. J. Wuhan Univ. Technol. - Mater. Sci. Ed. 25(1): 142-146.

Zhou X., Yang H. and Wang F. 2012. Investigation on the inhibition behavior of a pentaerythritol glycoside for carbon steel in 3.5% NaCl saturated Ca $(OH)_2$ solution. Corros. Sci. 54: 193-200.